Int. J. Multiphase Flow Vol. 11, No. 2, pp. 121–132, 1985
Printed in the U.S.A.

0301-9322/85 $3.00 + .00

THE EFFECT OF DUST AND WATER DROPLETS ON THE RELAXATION ZONE DEVELOPED BEHIND STRONG NORMAL SHOCK WAVES

O. IGRA, G. BEN-DOR and Z. RAKIB
The Pearlstone Center for Aeronautical Engineering Studies, Department of Mechanical Engineering, Ben-Gurion University of the Negev, Beer-Sheva, Israel

(*Received* 27 *November* 1983; *in revised form* 29 *July* 1984)

Abstract—The propagation of strong normal shock waves into a quiescent suspension composed of argon gas, water droplets and solid dust particles is studied. For evaluating the flow behaviour in the relaxation zone, the conservation equations for a steady, one-dimensional suspension flow are formulated and solved numerically. The solution indicates that the presence of water droplets and dust particles has a significant effect on the flow inside the relaxation zone and on the eventually reached post-shock suspension equilibrium state. Higher pressures and temperatures are obtained in the suspension as compared with a similar pure argon case. Changes in the physical properties of the dust have noticeable effect on the dust behaviour in the relaxation zone. However, these changes have only small effect on either the behaviour of the gaseous phase or the eventually reached post-shock suspension equilibrium state.

1. INTRODUCTION

Strong shock waves can be generated in the Earth's atmosphere by lightning, chemical explosives or nuclear devices. Since the Earth's atmosphere may contain a variety of small solid particles (dust) and water droplets, it is of interest to assess the effect of these additives on the post-shock flow, in particular at the relaxation zone developed behind the shock front. Throughout this relaxation zone nonequilibrium processes, leading from the frozen flow conditions (reached immediately behind the shock front) toward the eventually reached post-shock equilibrium, take place. Ben-Dor & Igra (1982) studied the case of a strong normal shock wave propagating into quiescent dusty argon gas. Rakib *et al.* (1984) solved the case of argon seeded with water droplets. The purpose of the present paper is to combine these two works and thereby extend the solution to cover the case of a strong normal shock wave propagating into a quiescent suspension composed initially of three phases: gas (for simplicity argon gas is used), solid (dust particles) and liquid (the water droplets). The solution of the conservation equations is conducted inside the relaxation zone, shown schematically in figure 1. Inside this zone interactions between the various components of the suspension takes place. Unique temperature for the gaseous phase is reached via collisional-radiative processes. Thermal and kinematic equilibrium among the different phases of the suspension is reached via viscous and heat transfer interactions. This equilibrium state is reached at the end of the relaxation zone.

The conservation equations for a gas-solid suspension (argon and dust) are given in Ben-Dor & Igra (1982) and for a gas-liquid suspension (argon and water droplets) in Rakib *et al.* (1984). Since the conservation equations for a suspension composed of argon gas, water droplets and dust particles could easily be derived from the combination of the equations given in the above-mentioned papers, it is felt that a detailed derivation is not needed. Those interested in this derivation and/or the final form of the conservation equations appropriate to the present case can obtain them from the authors.

The conservation equations were solved numerically throughout the relaxation zone. The solution was conducted up to the end of the longest of the following three lengths:

(i) Thermal relaxation length for the plasma L_{T_e}. L_{T_e} is the distance from the shock front to the point at which $(T - T_e)/T \leq 0.01$.

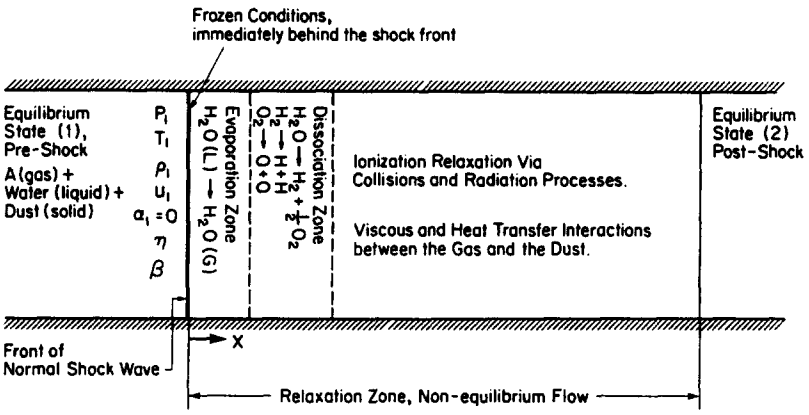

Figure 1. Illustration of the investigated flow field.

(ii) Thermal relaxation length for the suspension L_τ. L_τ is the distance from the shock front to the point at which $(T - \tau)/T \leq 0.02$.

(iii) Kinematic relaxation length for the suspension L_v. L_v is the distance from the shock front to the point at which $(v - u)/u \leq 0.02$.

T, T_e and τ are the gas heavy particles (atoms and ions) temperature, the electron gas temperature and the dust temperature, respectively.

The solution was obtained for shock-wave Mach numbers within the range $12 \leq M \leq 16$ and for preshock conditions of $p_1 = 5$ torr; $T_1 = 300$ K; $\eta = 0$, 0.1 and 0.2; $\beta = 0$, 0.001, and 0.01 and for dust particles having the following properties: $d = 1.2$, 1.5 g/cm^3; $D = 0.0001$, 0.0005 cm; $C = 5 \times 10^6$, 10^7 erg/g/K; $\epsilon = 0$,1. p_1 and T_1 are the preshock pressure and temperature, respectively. β and η are water droplets to argon gas mass ratio and dust to argon gas mass ratio, respectively, D, d, C and ϵ are the dust particle diameter, density, specific heat capacity and emissivity, respectively.

2. RESULTS AND DISCUSSION

For demonstrating the effect of the water droplets and the solid dust particles on the post-shock suspension properties, the conservation equations were solved using a few different values for the shock-wave Mach number (which is equal to the preshock flow Mach number M, when the shock wave is brought to rest), water droplet mass concentration (β), dust mass concentration (η), dust particle diameter (D), dust particle density (d), dust specific heat capacity (C) and dust emissivity (ϵ). The solution was conducted for a suspension that might be generated in a shock tube, i.e. $12 \leq M \leq 16$, $T_1 = 300$ K and $p_1 = 5$ torr. For brevity, only the results obtained for $M = 15$ are shown here. The values of β, η, D, d, C and ϵ specified in the last paragraph of section 1 are used. First, the effect of water droplets and/or dust mass concentrations on the post-shock flow is discussed. Thereafter, the influence of the physical parameters of the dust particle on the post-shock flow is shown.

For studying the effect of the water droplets and dust mass concentration on the post-shock flow, the following values for the dust physical parameters were used: $D = 0.0005$ cm, $d = 1.5$ g/cm^3, $C = 10^7$ erg/g/K and $\epsilon = 1$. The obtained results are shown in figures 2 to 6. The following notation is used in these figures:

A: indicating that $\beta = 0$ and $\eta = 0$,

B: indicating that $\beta = 0.001$ and $\eta = 0.1$,

C: indicating that $\beta = 0.01$ and $\eta = 0.1$,

D: indicating that $\beta = 0.01$ and $\eta = 0.2$.

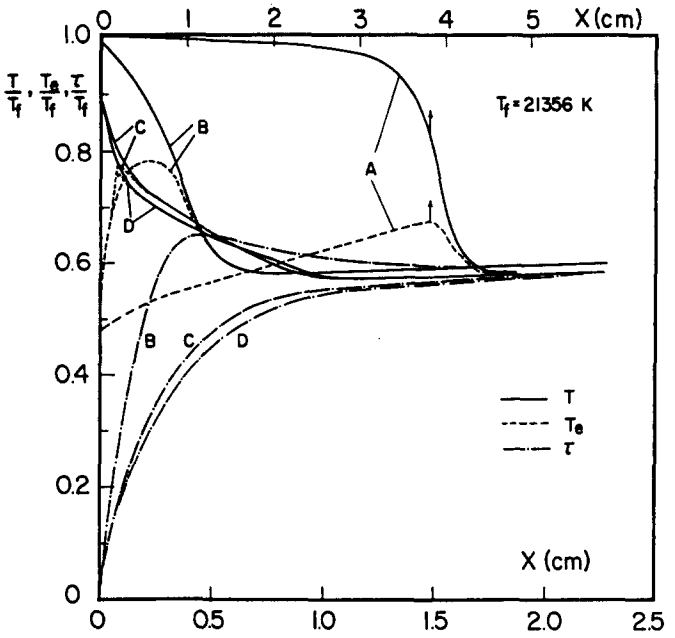

Figure 2. Variations in the gas temperature T, the electron gas temperature T_e and the dust temperature τ in the relaxation zone.

The temperature variations in the relaxation zone, for different values of β and η, are shown in figure 2. The temperature is normalized by the post-shock frozen value (T_f = 21,356 K for M = 15). Since the relaxation lengths for the suspension are much shorter than that obtained for the pure gas (case A where $\beta = \eta = 0$), two length scales are used in figure 2. The upper scale should be used for the pure argon (case A) while the lower scale belongs to the suspension (cases B, C and D). As could be expected, increasing the water droplet concentration causes a decrease in the gas temperature behind the shock front. This reduction in the post-shock gas temperature is closely associated with the energy withdrawn from the argon gas by the water droplets while evaporating and dissociating to their basic elements (H and O). Obviously, the higher the water droplet concentration is, the more

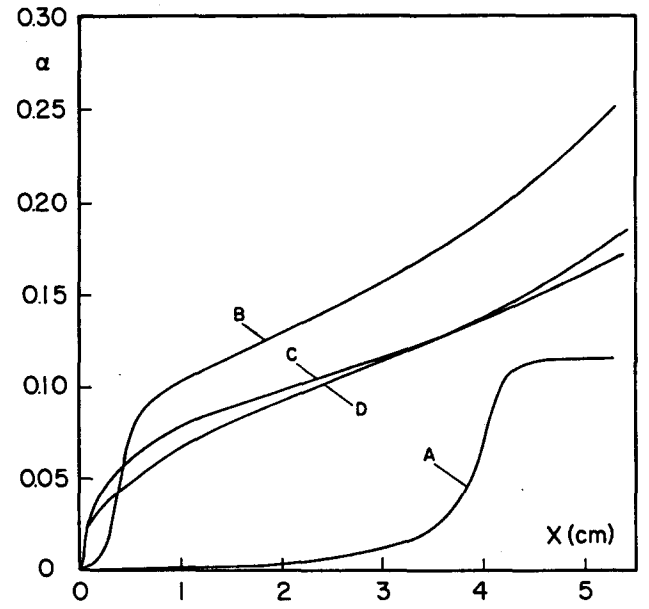

Figure 3. Variations in the degree of ionization in the relaxation zone.

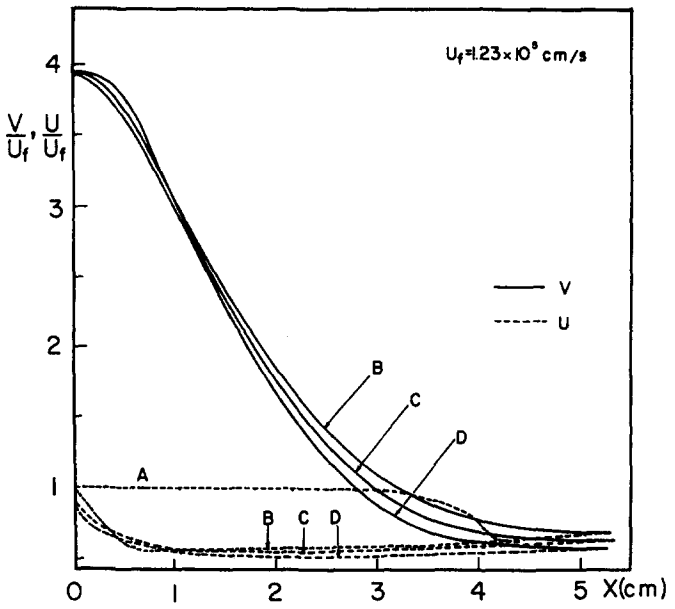

Figure 4. Variations in the flow velocity u and the dust velocity v in the relaxation zone.

energy is consumed in the water droplets evaporation and dissociation. In figure 2 it is manifested by lower gas temperature along curves C and D (where $\beta = 0.01$) as compared to curve B (where $\beta = 0.001$).

In addition to lowering the gas temperature behind the shock front, the presence of the water droplets has a significant effect on the extent of the plasma thermal relaxation zone. For a pure argon, T_e reaches T after a distance of about 4.5 cm, see curve A in figure 2. This distance is reduced to less than 1 cm when water droplets are introduced; curves B, C and D in figure 2. The effectiveness of these additives (impurities H and O) in shortening the plasma thermal relaxation zone was noted earlier by Morgan & Morrison (1965) and more recently by Glass & Liu (1978). It stems from the fact that they provide a source for generating free electrons at a faster rate than is possible from a pure argon. A more detailed explanation is given while discussing the variations in the plasma degree of ionization.

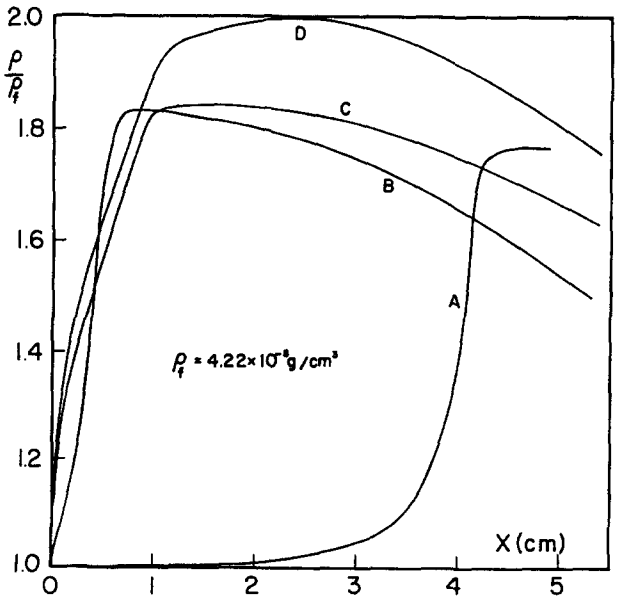

Figure 5. Density variations in the relaxation zone.

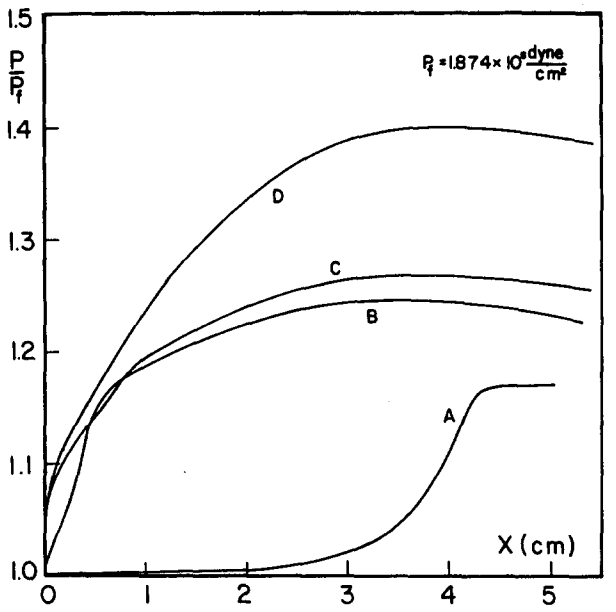

Figure 6. Pressure variations in the relaxation zone.

As could be expected for an ionizing shock wave, throughout the relaxation zone T_e is lower than T. The largest difference $T - T_e$ is associated with the pure argon (case A); this difference obtains smaller values as β increases. T_e lags behind T since the gas temperature behind the shock wave is just sufficient for partial ionization of the gas, especially for the pure argon case. As a result, most of the available thermal energy is consumed in the ionization process. Therefore, the produced free electrons will have a fairly low kinetic energy, i.e. low T_e. With increasing values of β more hydrogen and oxygen atoms become available. Since a smaller amount of energy is required for their ionization (as compared with argon atoms), the temperature of the free electrons, generated by ionizing the H or O atoms, will be closer to the gas temperature T.

The effect of the dust concentration on the suspension thermal relaxation is also shown in figure 2. While a thermal equilibrium between the electron gas and the heavy particle gas (atom and ions) is reached via collisional-radiative processes, the dust temperature is raised towards the appropriate post-shock equilibrium suspension temperature via conductive and radiative heat transfer from the gas to the dust. It is apparent from figure 2 that it takes longer time (and distance) to reach thermal suspension equilibrium ($T \simeq \tau$) as compared with thermal plasma equilibrium ($T \simeq T_e$). As the dust concentration increases, the total dust mass increases. Since the dust has a constant specific heat capacity and the initial dust temperature, for all cases, is the same ($\tau = 300$ K), it should be expected that longer times (and distances) will be required for heating a large mass of dust as compared with a smaller dust concentration. This is confirmed in figure 2. In case B ($\beta = 0.001$ and $\eta = 0.1$) the gas temperature, immediately behind the shock front, is relatively high (due to the low water droplet concentration) and the dust concentration is relatively low. As a result, intense dust heating takes place and τ overshoots T inside the relaxation zone. After a distance of about 1.5 cm (measured behind the shock front) τ eventually merges with T and a thermal suspension equilibrium is reached; case B in figure 2. In case C the post-shock gas temperature is lower than that of case B due to the increase in the water droplet concentration (now $\beta = 0.01$). This lowering in the gas temperature has a noticeable effect on τ; now τ increases monotonically towards T (no overshoot) and at a slower rate than that of case B. This results in a longer thermal suspension relaxation; it takes about 2 cm (behind the shock front) until τ reaches T. Increasing the dust concentration from $\eta = 0.1$ to $\eta = 0.2$

(case *D* in figure 2) results in a slower dust heating and a longer thermal relaxation length for the suspension.

It is evident from figure 2 that the highest post-shock equilibrium temperature is associated with case *B* while the lowest belongs to the pure argon, case *A*. (Note that the distance behind the shock front covered in cases *B*, *C* and *D* is only 2.5 cm while case *A* covers 5 cm; should all have been shown on the same length scale, 5 cm, it would have been clearer that the lowest post-shock equilibrium temperature belongs to case *A*).

Since the degree of ionization is strongly temperature dependent, small differences in both T and/or T_e between the four cases (*A*, *B*, *C* and *D*) would have a marked effect on the obtained values for α. This is indeed the case as is apparent from figure 3. The highest degree of ionization is experienced in case *B* where the highest values for T_e and for the post-shock equilibrium temperature are observed. The lowest values of α are associated with the case having a relatively low T_e and post-shock equilibrium temperature, i.e. case *A*.

It is of interest to note that case *A* in figure 3 exhibits a different ionization pattern (rate) than cases *B*, *C* and *D*. In case *A* the two steps ionization process as described by Wong & Bershader (1966) for argon is clearly seen. Initially there are practically no free electrons in the argon gas behind the shock front. As a result the only ionization process is the inefficient argon atom-atom inelastic collisions (Wong & Bershader 1966). In figure 3, the region where ionization is controlled by this process is represented by the very slow increase in α; starting at $X = 0$ and up to about $X = 2.75$ cm. At the end of this region ($X \simeq 2.75$ cm) sufficient amount of free electrons have been produced by the relatively inefficient atom-atom inelastic collisions to enable the more effective electron-atom inelastic collisions to become the dominant ionization process (Wong & Berhsader 1966). At this point the second step in the ionization process, typified by an avalanche in free electron production, starts. In figure 3 (case *A*) this step is represented by the very fast increase in α between $X \simeq 2.75$ and up to $X \simeq 4.25$. Thereafter, an equilibrium state is reached.

The introduction of water droplets into the argon gas significantly alters this two-steps ionization process because the added elements (H and O) are ionized much faster than the argon atoms due to the following reasons:

(i) The ionization potential of the hydrogen and oxygen atoms are 13.6 and 13.5 eV, respectively, as compared with 15.75 eV for the argon atom. (Similarly, the excitation energy, for the first excited atomic state, for H and O is lower than that for A.)

(ii) The excitation and ionization collision cross sections of the hydrogen atoms are significantly larger than those of the argon atoms (Glass & Liu 1978).

Therefore, the initial slow ionization rate typical to pure argon (case *A* in figure 3) will practically disappear when water droplets are added as is evident in cases *B*, *C* and *D* in figure 3. As could be expected, increasing the water droplet concentration resulted in a faster ionization (since more H atoms become available and they provide the source for the initial critical amount of free electrons). This is evident from comparing cases *C* and *D* with case *B*. However, since the increase in β reduces the gas temperature in the relaxation zone (since more energy is withdrawn from the gas to enable the water droplets evaporation and dissociation), lower degree of ionization are experienced in cases *C* and *D*, as compared with *B*; in spite of their faster initial ionization rate, see figure 3.

The velocity variations in the relaxation zone are shown in figure 4. Both the dust (v) and the gas (u) velocities are normalized by the frozen gas velocity obtained immediately behind the shock front. The dust enters the relaxation zone with a relatively high velocity. (The dust velocity is equal to the shock velocity since for bringing the moving shock wave into a stationary position a velocity equal to the shock-wave velocity, but in the opposite direction is imposed on the entire flow field.) The dust is decelerated to the appropriate post-shock equilibrium suspension velocity through viscous interaction with the gas. It is apparent from figure 4 that increasing the dust concentration results in a decrease in the post-shock

equilibrium suspension velocity (see cases C and D in figure 4). Similar effect is found when the water droplet concentration is increased: higher post-shock equilibrium suspension velocity is associated with the lower water droplet concentration (compare case B, where $\beta = 0.001$, with C where $\beta = 0.01$, in figure 4). It is also apparent from figure 4 that a longer distance is passed until an equilibrium velocity is reached in the suspension cases ($\beta > 0, \eta > 0$), as compared with the pure argon case ($\beta = \eta = 0$). It is evident from Figs 2 and 4 that the suspension kinematic relaxation zone (distance passed until $v \simeq u$) is always longer than the thermal relaxation zones (distances passed until $T_e \simeq T$ and $\tau \simeq T$), in agreement with Ben-Dor & Igra (1982) findings for dusty shocks in argon.

The variations in the gas density, inside the relaxation zone, are shown in figure 5. The density is normalized by the frozen density as predicted by the Rankine-Hugoniot relations. Like the observed variations in α, here again the density variations for the various suspensions (cases B, C and D) are different than that observed in the pure argon (case A). In the latter, the changes in the gas density behind the shock front are initially small (increase) to be followed by a fast increase in ρ (starting at a distance of about 3.5 cm behind the shock front). This fast increase in ρ is terminated when an equilibrium state is reached. On the other hand, the suspension (cases B, C and D) experiences a very fast increase in ρ, starting immediately behind the shock front, see figure 5. Once a maximum value for ρ is reached, a slow decline in ρ follows for all the suspension cases. Ben-Dor & Igra (1982) reported a similar fast increase in ρ, at the early part of the relaxation zone, for dusty shocks in argon. However, when water droplets are not included, this initial fast increase in ρ is continued to a different conclusion. The density continuously increases until an equilibrium state is reached (see figure 4 in Ben-Dor & Igra 1982). It should therefore be concluded that the decline in ρ at the latter part of the relaxation zone shown in figure 5, is due to the water droplet presence. Increasing either β or η results in a higher post-shock gas density. Larger increases in ρ are associated with increasing η's as is evident from comparing curves B and C of figure 5 (in both B and C, $\eta = 0.1$ while β is increased tenfold, from 0.001 in B to 0.01 in C), with curves C and D (where $\beta = 0.01$ and η is only doubled, from $\eta = 0.1$ in curve C to $\eta = 0.2$ in D). The reason that cases B, C and D do not start from $\rho/\rho_f = 1$, as does case A, is due to the corrections made to the post-shock frozen flow properties to account for the water droplets evaporation and the dissociation to their elements (H and O).

The pressure variations, in the relaxation zone, are shown in figure 6. They follow a pattern similar to that exhibited by the gas density; i.e. the suspension pressure increases with increasing either β or η. Larger increases are associated with increasing the dust mass concentration as compared with increase in β. Like the behaviour noticed in ρ, for the pure argon (case A), the pressure increase is initially very moderate. A rapid increase in the pressure is noticed only at the latter part of the relaxation zone. On the other hand, for the suspensions (cases B, C and D) very large increases in pressure are noticed at the early part of the relaxation zone, leading to a maximum value; thereafter a moderate decline is witnessed, see figure 6. Again, the difference in the initial values for p, obtained for the different cases, is due to the corrections made to the post-shock frozen flow properties to account for evaporation and dissociation of the water droplets.

In summary, the introduction of either water droplets or dust particles to the argon resulted in an increase in the post-shock flow pressure and density. The higher β or η, the larger p and ρ becomes; however, increases in η cause larger increases in both p and ρ, than increases in β. The opposite is true for the post-shock equilibrium suspension velocity. Increasing either β or η results in a lower velocity. The lowest post-shock equilibrium temperature and degree of ionization are obtained for the pure argon case. For the suspension, both the post-shock equilibrium temperature and the plasma degree of ionization reduces as either β or η increases. The highest values for α and T_{eq} are associated with the lightest loading (case B where $\beta = 0.001$ and $\eta = 0.1$).

Now the effect of dust physical properties on the flow in the relaxation zone is studied. For this purpose the loadings β and η were fixed at $\beta = 0.01$ and $\eta = 0.1$. The results obtained for variations in the flow temperature, velocity, density and pressure are shown in figures 7 to 10. The following notation is used in these figures:

a: indicating that $D = 0.0005$ cm, $d = 1.5$ g/cm^3, $C = 10^7$ erg/g/K and $\epsilon = 1$
b: indicating that $D = 0.0001$ cm, $d = 1.5$ g/cm^3, $C = 10^7$ erg/g/K and $\epsilon = 1$
c: indicating that $D = 0.0005$ cm, $d = 1.2$ g/cm^3, $C = 10^7$ erg/g/K and $\epsilon = 1$
d: indicating that $D = 0.0005$ cm, $d = 1.5$ g/cm^3, $C = 5 \times 10^6$ erg/g/K and $\epsilon = 1$
e: indicating that $D = 0.0005$ cm, $d = 1.5$ g/cm^3, $C = 10^7$ erg/g/K and $\epsilon = 0$.

From the temperature signatures, shown in figure 7, it is suggested that T and T_e are unaffected by dust physical properties. In the obtained numerical results there were small changes in both T and T_e due to changes in either D, d, C or ϵ. However, these changes were very small in comparison with those obtained for the dust temperature τ; their inclusion would have resulted in a thick (smeared) curve for the T and T_e. Therefore, it was decided to show both T and T_e as a light line, passing through the center of the group of individual lines laying closely together.

The rate at which the dust particles are being heated depends on the temperature difference $T - \tau$, the dust particle mass m, and its specific heat capacity C. For all cases (*a* to *e*) the initial dust temperature (immediately behind the shock front) is 300 K. Since T is hardly affected by the dust physical properties, practically the same initial temperature difference will be experienced in all the five cases (*a* to *e*). Cases *a* to *c* and case *e* represents dust particles with the same specific heat capacity, $C = 10^7$ erg/g/K. Therefore, the fastest rate of dust heating is expected for the lightest dust particles; this indeed is the case as is evident from figure 7 where the fastest heating is experienced by the smallest dust particles (case *b* where $D = 0.0001$ cm). It should be noted that the dust particle mass m, depends on both its diameter D and density d; $m = 1/6\ \pi D^3 d$. However, while m is linearly dependent upon d, m is proportional to the third power of D. This explains why case *b* experiences the fastest heating and in case *c* the dust is being heated faster than in case *a*. (In case *c*, $d = 1.2$ g/cm^3 while in case *a*, $d = 1.5$ g/cm^3; all other properties are the same in both cases.) Case *d* represents the dust particles with the lowest specific heat capacity, as a result this dust will

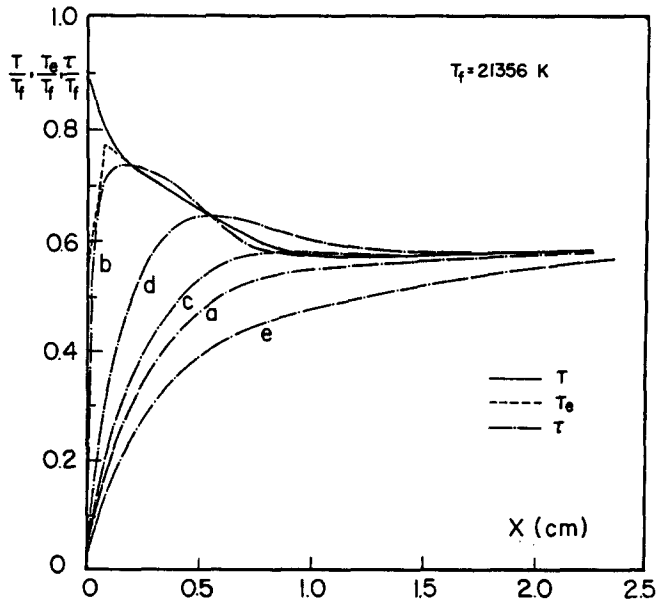

Figure 7. Variations in the gas temperature T, the electron gas temperature T_e and the dust temperature τ, in the relaxation zone.

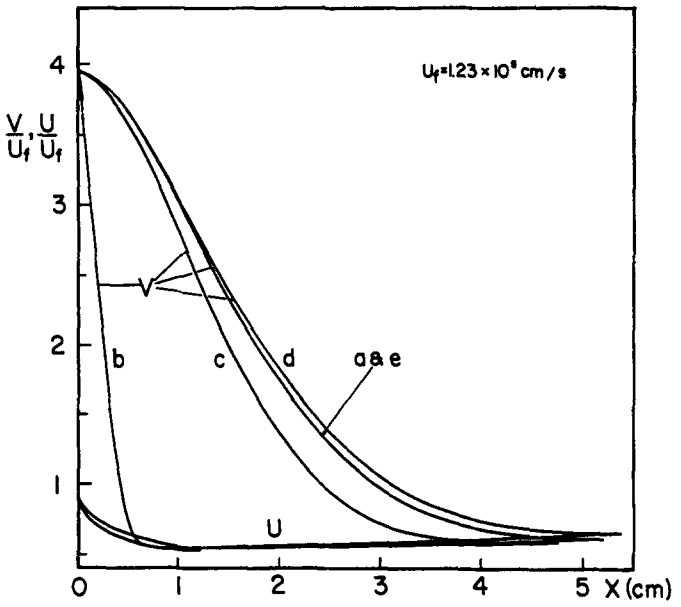

Figure 8. Variations in the flow velocity u and the dust velocity v in the relaxation zone.

be heated very fast and τ overshoots T in the relaxation zone, see figure 7. (Smaller overshooting of τ relative to T is experienced when the dust mass is relatively small, cases b and c.)

The dust particles are heated by the gas through convective and radiative heat transfer. In case a to d the dust particles are assumed to behave like a black body ($\epsilon = 1$); in case e no radiative heat transfer takes place ($\epsilon = 0$). As could be expected when the heat transfer is limited to convection only, longer time (and distance behind the shock front) will be required until τ reaches T, as is evident from case e in figure 7.

The effect of the dust physical properties on the suspension velocities is shown in figure 8. It has a minor effect on the gas velocity u, however, it significantly affects the dust velocity v. The dust deceleration results from the drag force it experiences. From the equation describing the momentum exchange gas-dust (see equation 11 in Ben-Dor & Igra 1982) it is

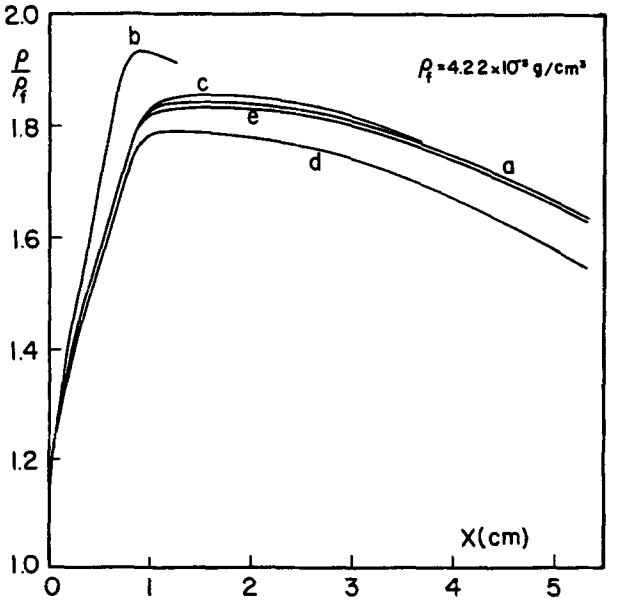

Figure 9. Density variations in the relaxation zone.

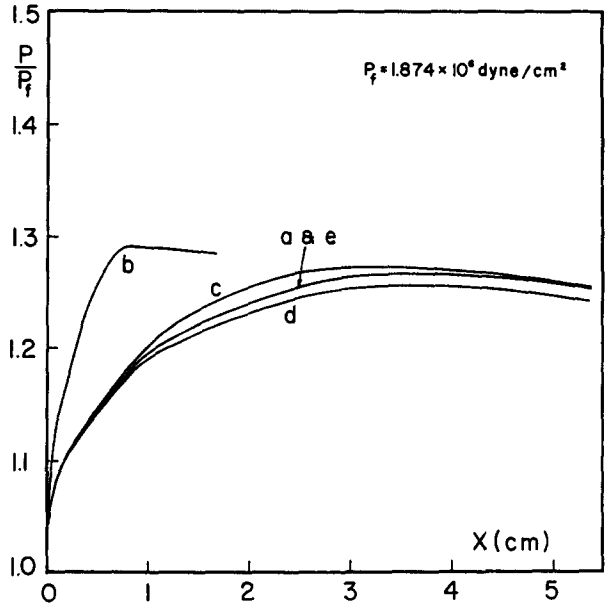

Figure 10. Pressure variations in the relaxation zone.

apparent that dv/dx is inversely proportional to either D or d; i.e. decreasing the dust diameter or density will increase its deceleration. It is evident from figure 8 that the fastest deceleration is associated with the smallest values of D and d used; cases *b* and *c*, respectively. In case *b* faster deceleration is experienced than in case *c* due to the following reasons:

(i) The reduction in the dust particle diameter in case *b*, relative to that of cases *a* and *c* to *e* is by a factor of 5 (0.0001 cm instead of 0.0005 cm) while the reduction in the dust particle density in case *c*, relative to the value used in cases *a*, *b*, *d* and *e* is only by a factor of 1.1538 (1.2 g/cm^3 instead of 1.5 g/cm^3).

(ii) Changes in either D or d affect the dust particle mass. However, while m depends linearly on d, its dependence upon D is to the third power, i.e. the dust particle mass in case *b* is significantly smaller than that of case *c*. The drag force acting on the dust particle is linearly dependent on its frontal cross section ($\pi D^2/4$); it will be smaller in case *b* as compared with the drag force of case *c*. However, the reduction in mass is much larger than the reduction in the drag force (D^3 as compared with D^2) and as a result faster deceleration is expected in case *b*.

As could be expected changes in the dust specific-heat capacity have minor effect on the dust velocity, changes in the dust particles emissivity have no effect on v; see cases *a*, *d* and *e* in figure 8.

The effect of the dust physical properties on the gas density, in the relaxation zone, is shown in figure 9. The smaller the dust particle is, the higher the gas density becomes. This should not be surprising since for a steady one-dimensional flow ρu = const. Recall that the lowest gas velocity was obtained for the case having the smallest dust particles, case *b* in figure 8. Therefore, the highest values of ρ should be expected for this case (case *b*, figure 9). On the other hand, the highest post-shock equilibrium velocity was associated with case *d* (see figure 8) and it should therefore be expected that the lowest ρ's will be associated with case *d*; as is evident from figure 9. Changes in the dust particle density and emissivity have only a mild effect on the obtained values for ρ (compare *a*, *c* and *e*)

The effect of the dust physical properties on the suspension pressure is shown in figure 10. The fastest rise in pressure, behind the shock front, is associated with the smallest dust particles (case *b* in figure 10 where D = 0.0001 cm). This fast rise in pressure stems from the

fast deceleration typical to this case (curve *b*, figure 8). However, the post-shock equilibrium suspension pressure is only mildly affected by the dust particle mass or its specific-heat capacity. It is unaffected by changes in the dust particle emissivity. Similar post-shock equilibrium pressures are reached in all five cases.

In summary, changes in the dust particle mass (by either changing its diameter or density) have a marked effect on the dust particle rate of heating and its deceleration thereby strongly affecting the extent of the suspension thermal and kinematic relaxation zones. These changes have minor effect on the obtained post-shock equilibrium temperature and velocity. It also has only a small effect on the post-shock density and pressure. Changes in the dust particle specific-heat capacity and its emissivity affect mainly the dust rate of heating and thereby the extent of the suspension thermal relaxation zone. While changes in C have only a small effect on the other suspension properties, changes in ϵ have practically no effect on the suspension pressure and velocity.

It could be asked at this point why changes in the dust particle mass (via changes in either D or d) have small effect on the flow properties at the latter part of the relaxation zone (especially small effect on ρ and p) while changes in the dust cloud mass (via changes in η) have a marked effect on the flow inside the relaxation zone, including the eventually obtained equilibrium state.

While changing the dust particle mass, by definition the total dust mass remains unchanged since, in the results shown in figures 7 to 10, $\eta = 0.1$. (The total dust mass is always 9.09% of the entire suspension mass.) Changes in the dust particle mass will affect the drag force acting on it, its deceleration and its rate of heating as was shown before (figures 7 and 8). However, since the total dust mass is remained unchanged ($\eta = 0.1$) the effect on the post-shock equilibrium values is minor. This is not the case in the results shown in figures 2 to 6. In these results cases of $\eta = 0.1$ and $\eta = 0.2$ are compared; i.e. the total dust mass is increased from 9.0% of the suspension mass (when $\eta = 0.1$) to 16.53% of the suspension mass (when $\eta = 0.2$). This of course will affect the eventually reached post-shock equilibrium state.

CONCLUDING REMARKS

The conservation equations for the flow field developed behind a strong normal shock wave propagating into a quiescent three-phase suspension (composed of argon gas, water droplets and dust), were formulated and solved.

The solution indicated that the presence of water droplets and dust particles has a significant effect on the flow in the relaxation zone. The evaporation and dissociation of the water droplets to their basic elements is completed within a relatively short distance behind the shock front, due to the elevated post-shock temperature. Thereafter, the preshock three-phase suspension (argon-water droplets-dust) is reduced to a two-phase suspension (a gas mixture A + H + O, and solid dust particles). Since singificant amounts of energy are consumed in the evaporation and dissociation of the water droplets, the flow properties at the beginning of the ionization-relaxation zone are different from those obtained immediately behind the shock front. In a pure argon case the ionization rate is relatively slow since it is controlled initially by the inefficient argon atom-atom inelastic collisions. This is no longer the case for the suspension. Due to presence of hydrogen (and oxygen) atoms, ionization commences faster since the H atoms are ionized faster than the A atoms. The different ionization rates are clearly visible in the α versus x plot (figure 3).

While the interactions between the three elements of the gaseous phase (A, H and O) are limited to collisional-radiative processes, the interactions between the gaseous phase and the dust (solid) are via viscous and heat transfer. Generally, the latter take longer time than the former, resulting in a relatively short thermal relaxation zone for the plasma as compared with the extent of the suspension thermal and kinematic relaxations. The presence of water

droplets and dust particles results in an increase in the rate at which the flow properties are changed behind the shock front. It also affects the eventually reached equilibrium state. Their presence has a marked effect on the post-shock pressure and degree of ionization and a milder effect on the post-shock temperature and velocity (as compared with a similar pure argon case). Larger changes (increases) in the post-shock flow properties are associated with increases in the dust mass concentration as compared with changes associated with increases in the water droplet mass concentration.

Changes in the dust particle mass (via changes in its diameter or density) have a pronounced effect on the dust deceleration and its rate of heating. However, these changes have only a small effect on the eventually reached equilibrium values of u and T. It also has a mild effect on the post shock pressure and density. Changes in the dust particle specific-heat capacity and its emissivity affect mainly the dust rate of heating.

Acknowledgment–The financial assistance received from the U.S. government through its European Research Office of the U.S. Army under Grant No. DA JA 37-81-C-0499 is acknowledged with gratitude.

REFERENCES

BEN-DOR, G. & IGRA, O. 1982 The relaxation zone behind normal shock waves in a reacting dusty gas. Part 1, monatomic gases. *J. Plasma Phys.* **27**, 377–395.

GLASS, I. I. & LIU, W. S. 1978 Effects of hydrogen impurities on shock structure and stability in ionizing monatomic gases. Part 1, argon. *J. Fluid Mech.* **84**, 55–77.

MORGAN, E. J. & MORRISON, R. D. 1965 Ionization rates behind shock waves in argon. *Phys. Fluids* **8**, 1608–1615.

RAKIB, Z., IGRA, O. & BEN-DOR, G. 1984 The effect of water droplets on the relaxation zone developed behind strong normal shock waves. *ASME J. Fluid Engng.* **106**, 154–159.

WONG, H. & BERSHADER, D. 1966 Thermal equilibration behind an ionizing shock. *J. Fluid Mech.* **26**, 459–479.